

TIME SERIES ANALYSIS OF AMBIENT AIR CONCENTRATIONS IN ALEXANDRIA AND NILE DELTA REGION, EGYPT

El Raey M.^(a), E.A. Shalaby, Z. F. Ghatass and H. S. Marey

Department of Environmental Studies, Institute of Graduate Studies and Research (IGSR), Alexandria University, Alexandria, Egypt

(a) Elraey@ link.net

Data collected from the Air Monitoring Network of Alexandria and Delta (EEAA/EIMP-program), were analyzed. Emphasis is given to indicator pollutants PM₁₀, NO₂, SO₂, O₃ and CO. Two sites have been selected in Alexandria (IGSR and Shohada) and three sites in Delta region (Kafr Elzyat, Mansoura and Mahalla) for analysis of three years from 2000-2002. Box –Jenkins modeling has been used mainly for forecasting and assessing relative importance of various parameters or pollutants.

Results showed that, the autoregressive (AR) order for all series ranged from 0-2 except NO₂ at Mansoura site. Also the moving average order ranged from 0-2 except CO at IGSR site. Nitrogen dioxide and Ozone at IGSR site have the same ARIMA model which is (0, 1, and 2).

Cross correlation analysis has revealed important information on the dynamics, chemistry and interpretation of ambient pollution. Cross-correlation functions of SO₂ and PM₁₀ at IGSR sites suggest that, sulfur dioxide has been adsorbed on the surface of particulates which has an alkaline nature. This enhances the oxidation of sulfur dioxide to sulfate, which results in low levels of SO₂ in spite of the presence of sources.

(Keyword: Air pollution modeling, Box-Jenkins models and Air pollution indicators).

INTRODUCTION

In recent years, air quality has emerged as a major factor contributing to the quality of life in urban areas, especially in densely populated and industrialized areas. Air pollution control is needed to prevent the situation from becoming worse in the long run. On the other hand, short term forecasting of air quality is needed in order to take preventive and evasive action during episodes of airborne pollution. The trend in recent years has been to use more statistical methods instead of traditional deterministic modeling. A number of methods have been applied to time series of air pollutants for air quality forecasting (e.g. Kolehmainen et al., 2001, Kukkonen et al., 2003). Regression models used in air pollution studies do not deal with the mechanisms of atmospheric diffusion. They are empirical models and in many cases there is no theoretical or a priori information about the functional form of the effect of emissions, meteorology, or the past history of pollutant concentrations. Hence, from the conceptual point of view, stochastic models are preferred. Also, because of high autocorrelation of concentrations and the largely unknown causal mechanisms, a multiple regression model for air pollution, is likely to be unsatisfactory, unless a number of precautions are taken to ensure that the residuals are white noise (Milionis and Davies, 1994).

Stochastic models, on the other hand have been used successfully in air pollution modeling and atmospheric scientists are relatively familiar with the methodology associated with them. So, stochastic models are also preferred from the practical point of view. So, in the

absence of sufficient knowledge about the structure of causal factors, one may start to determine the current value of the series by using its own past behavior. No theoretical assumption is required and the character of the effect of the previous terms can be determined empirically from the available data. The only condition that needs to be imposed is that the series should be sufficiently long to allow reliable empirical identification of the character of this effect (Box and Jenkins, 1970).

It must be emphasized that, Box-Jenkins models are arbitrary. The final form of the noise component in an ARIMA model may contain AR or MA coefficients to which it may be difficult to assign a physical interpretation. However, it is certainly better to present a model which is correct, even though it cannot be fully explained, than to use a regression model which is technically wrong.

Our objective here is to apply univariate ARIMA models as a tool for forecasting and assessing the relative importance of various parameters or pollutants over Alexandria and Nile delta region.

2. MATERIALS AND METHODS

2.1 Data

Data were collected from the Air pollution Network of Alexandria and Delta (EEAA/EIMP). The data were collected in the city of Alexandria and Nile Delta region during the three years 2000-2002. Emphasis is given to indicator pollutants PM₁₀, NO₂, SO₂, O₃ and CO. Two sites have been selected in Alexandria (IGSR and Shohada) and three sites in Delta region (Kafr Elzyat, Mansoura and Mahalla) cities. The area types are listed in Table 1. and the location of sites are shown in Figure 1.

Table 1. Sites, area types and types of monitors for air pollution monitoring network in Alexandria at some Nile Delta cities

Station	Type of area	Pollutants
Alexandria	IGSR	Industrial/ Residential
	Shohada	Industrial
	Alexregional	Industrial/ Residential
Delta	Kafr Elzyat	Urban
	El-Mahalla	Urban
	El-Mansoura	Regional

2.2 Handling missing data

During the period of study there were several occasions with missing data at each site. It was necessary, therefore, to fill out missing data by values predicted from the linear trend regression. In this method, the program fits a least-squares regression line to the time series. The missing data are then replaced by values predicted by this regression line. This method implies that the most salient (or strongest) feature of the series is its linear trend across time. This was done with Statistica software (www.statsoft.com).

2.3 Model creation

Finding appropriate models for time series is a nontrivial task. There is a multistep model building strategy by Box and Jenkins. This process consists of three main steps which are:

- (i) model specification (or identification)
- (ii) model fitting (Estimation)
- (iii) model diagnostics

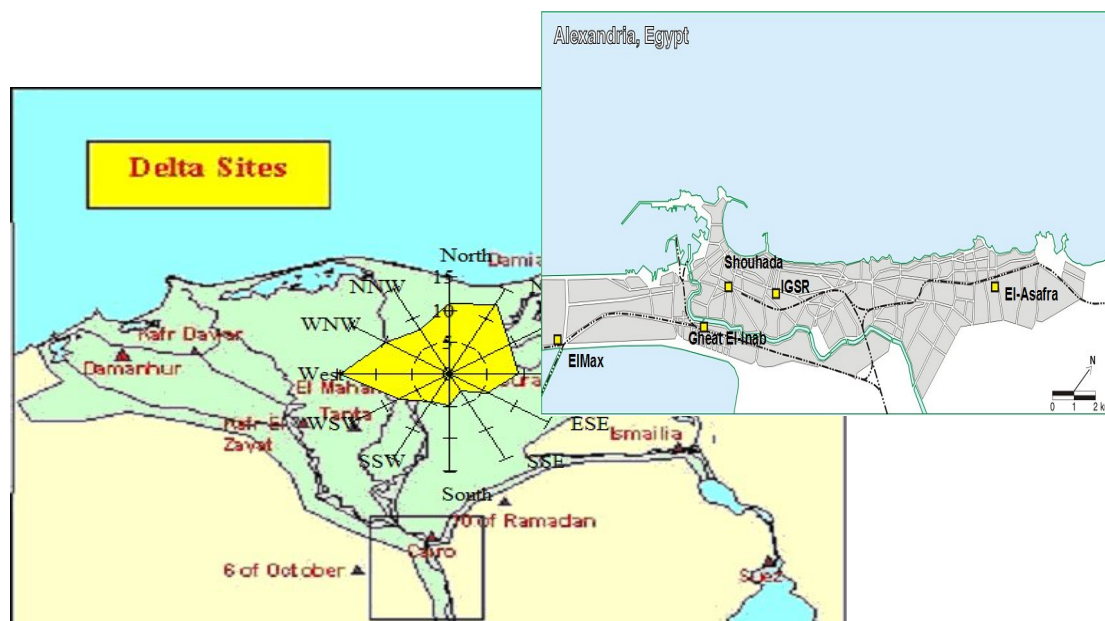


Figure 1. Location of air quality measurement stations in Alexandria and Nile Delta region.

(i) model identification

The major tools used in the identification phase are plots of the series, autocorrelation function (ACF) and partial autocorrelation function (PACF), where the patterns of ACF and PACF are used to identify a tentative model.

(ii) model fitting (Estimation)

Model fitting consists of finding the best possible estimates of unknown parameters within a given model. The estimation of parameters can be made by criteria such as least squares and maximum likelihood. The parameters are estimated, so that the sum of squared of residuals is minimized.

(iii) model diagnostics

The diagnosis is to examine the whiteness of the residuals. So, the analysis of ARIMA residuals was carried out by checking their independence, normality and constancy of the variance. Also, there is meta-diagnosis step, where the model is compared with other rival models (Milonis and Davies, 1994).

3. RESULTS AND DISCUSSIONS

The results of the three standard stages of model building strategy, namely identification, estimation, and diagnostic, will be discussed in details:

(I) Identification

Particulate matter (PM₁₀)

Visual inspection of time series plots suggests that the series have variance instability and needs to be differenced. The differenced data were carried out and ACF (autocorrelation function) and PACF (partial autocorrelation function) of the differenced PM₁₀ series are depicted in Figures 1., 2. and 3. for IGSR, Kafr Elzyat, and Mahala sites, respectively. It is worthy to mention that the data were stabilized after one difference only. Significant correlations at several lags were found to provide information about the ARIMA orders.

However a specific model is not immediately distinguishable. Many tentative models were tested, and several of them were found to be adequate. Meta-diagnostic analysis showed the best models that describe the PM10 series which are listed in Table 2. Where X_t refers to PM10 concentration at any time t , B is backshift operator; Φ and θ are autoregressive and moving average parameters, respectively and a_t is the white noise.

Table 2. ARIMA model for PM₁₀ of IGSR, Kafr Elzyat and Mahalla sites

Site	ARIMA (p,d,q)	Model
IGSR	(2,1,1)	$(1-\Phi_1B-\Phi_2B^2)(1-B)X_t = (1-\theta_1B)a_t$
Kafr Elzyat	(1,1,2)	$(1-\Phi_1B)(1-B)X_t = (1-\theta_1B-\theta_2B^2)a_t$
Mahalla	(0,1,1)	$(1-B)X_t = (1-\theta_1B-\theta_2B^2)a_t$

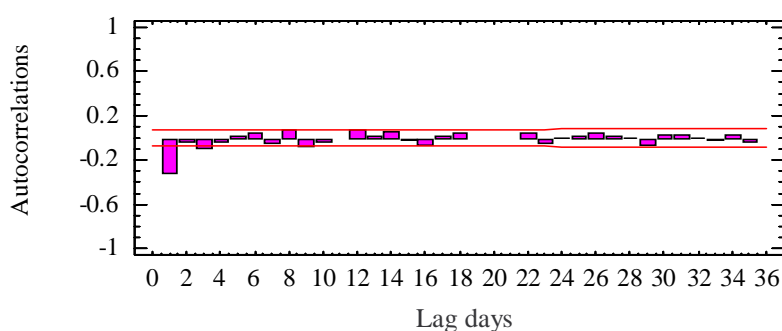


Figure 1a. ACF of daily average PM₁₀ after first difference of IGSR during the years (2000-2002)

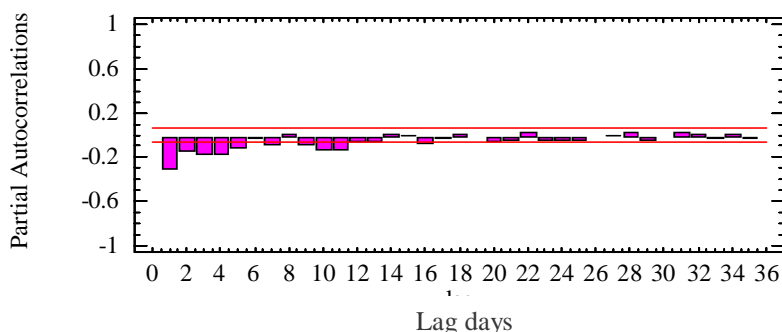


Figure 1b. PCF of daily average PM₁₀ after first difference during the years (2000-2002)

Nitrogen dioxide (NO₂)

The NO₂ series of IGSR site displays a negative trend than other sites which is also implied in the plot of ACF which reflects improvement in air quality. In order to test stationarity, the plots of autocorrelation (ACF) for NO₂ series of IGSR, Kafr Elzyat, and Mansoura sites are examined. The characters of these plots indicate that the NO₂ series are non stationarity and needs to be differenced. ACFs and PACFs (Figure 4a. - 6a. and Figure 4b. - 6b. of the differenced NO₂ data were made to confirm stationarity and assess tentative ARIMA models. Table 3. contains the best models that describe the NO₂ series as follows:

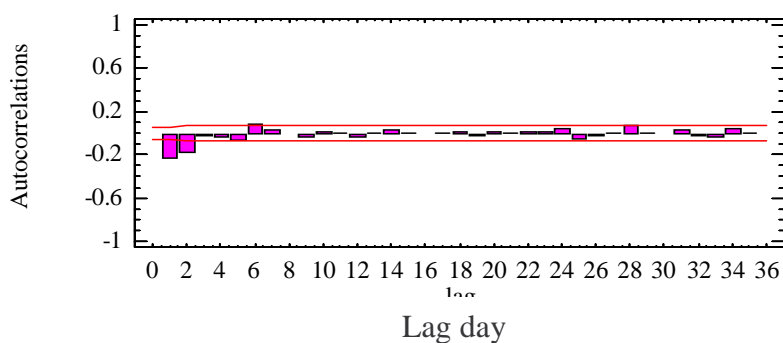


Figure 2a. ACF of PM₁₀ of KZ after first difference site for three years (2000-2002)

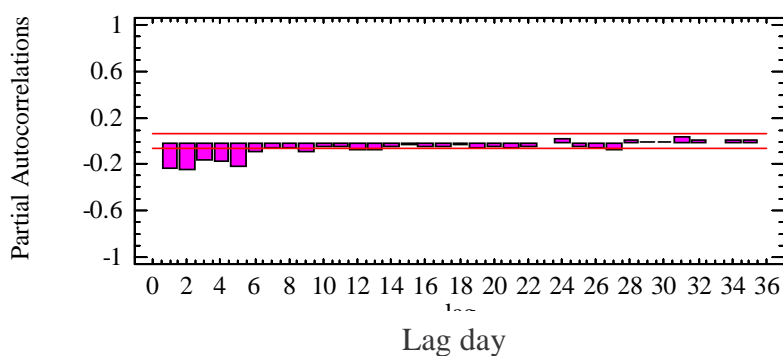


Figure 2b. PCF of PM₁₀ at KZ after first difference site for three years (2000-2002).

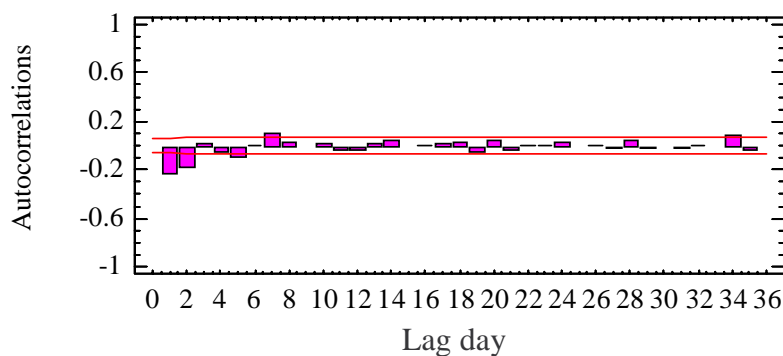


Figure 3a. ACF of PM₁₀ after first difference at Mahalla site during three years (2000-2002)

Table 3. ARIMA model for NO₂ of IGSR, Kafr Elzyat and Mansoura sites

Site	ARIMA (p,d,q)	Model
IGSR	(0,1,2)	$(1-\Phi_1B-\Phi_2B^2)(1-B)X_t = (1-\theta_1B)a_t$
Kafr Elzyat	(1,1,2)	$(1-\Phi_1B)(1-B)X_t = (1-\theta_1B-\theta_2B^2)a_t$
Mansoura	(5,1,1)	$(1-B)(1-\Phi_1B-\Phi_2B^2-\Phi_3B^3-\Phi_4B^4-\Phi_5B^5)X_t = (1-\theta_1B-\theta_2B^2)a_t$

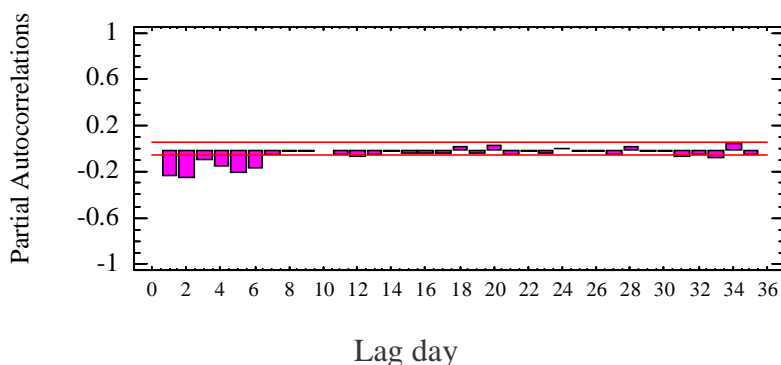


Figure 3b. PCF of PM₁₀ after first difference at Mahalla site during three years (2000-2002).

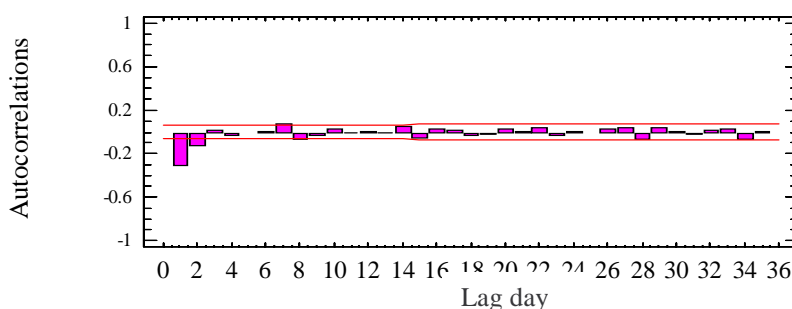


Figure 4a. ACF of NO₂ after first difference at IGSR site for three years (2000-2002)

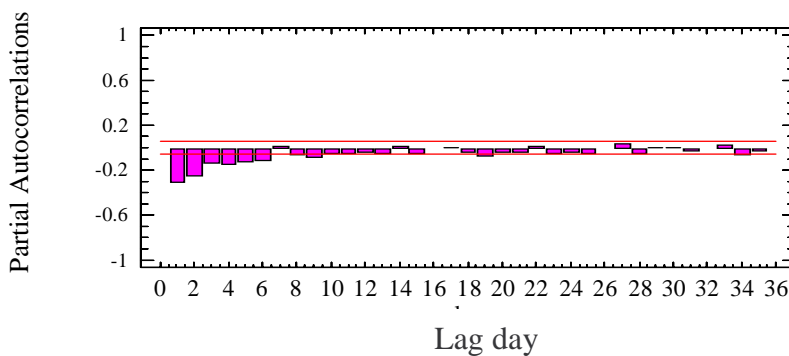


Figure 4b. PCF of NO₂ after first difference at IGSR site for three years (2000-2002).

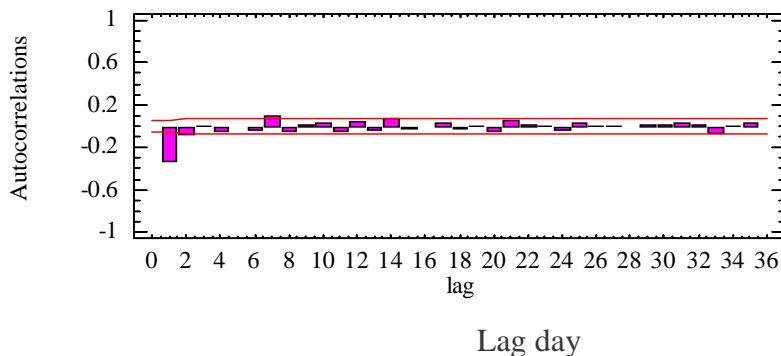


Figure 5a. ACF of daily average NO₂ at KZ site after first difference during three years (2000-2002)

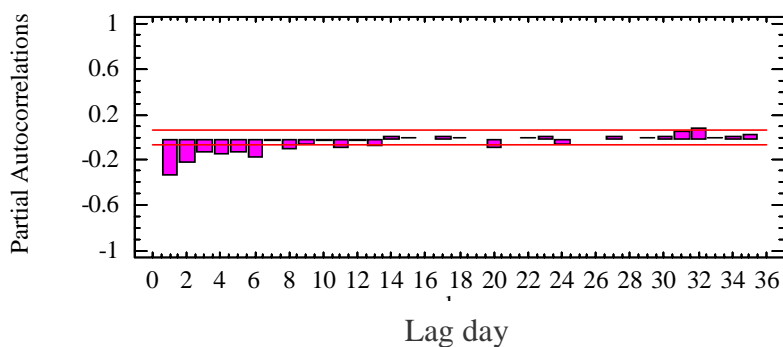


Figure 5b. PCF of daily average NO₂ at KZ site after first difference during three years (2000-2002)

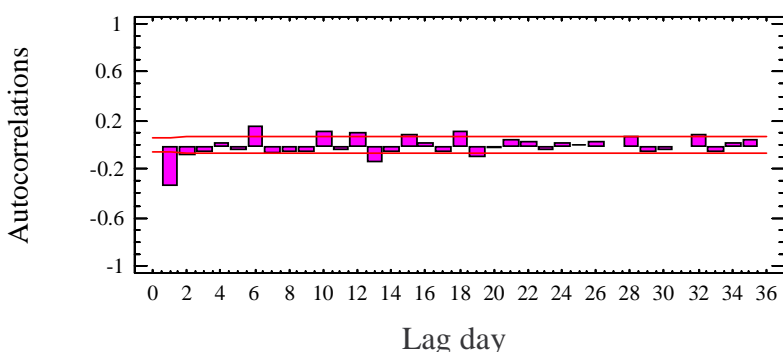


Figure 6a. ACF of daily average NO₂ at Mansoura site after difference during three years (2000-2002)

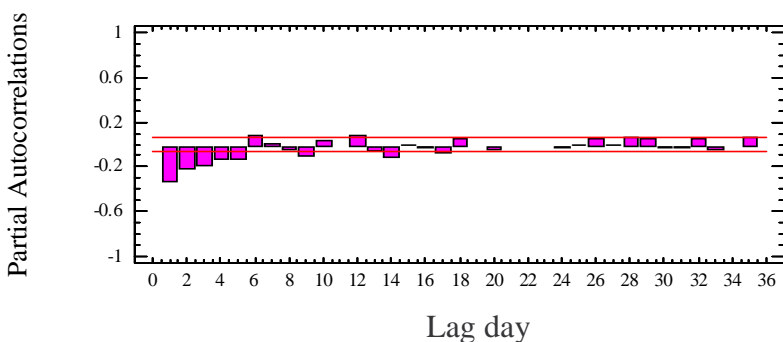


Figure 6b. PCF of daily average NO₂ at Mansoura site after first difference during three years (2000-2002)

Sulfur dioxide (SO₂)

SO₂ time series plots of IGSR and Kafr Elzyat appear to be stationary as verified by making ACFs. The ACFs of the time series values of SO₂ for IGSR and Kafr Elzyat die down quickly, then the time series data should be considered stationarity (constant in means and variance). While the ACFs of SO₂ series of Mahala and Mansoura sites die down slowly which supports the non stationarity. Thereafter they should be differenced to make them stationarity. Now according to the Box -Jenkins methodology, the behavior of ACF and PCF were examined to specify general ARIMA model. In case of SO₂ of IGSR the ACF dies down quickly whereas, the PCF has spikes at lag 1 and cuts off after lag 1 as shown in Figure 7a. and 7b. Thus the SO₂ series should be follow the AR(1) (autoregressive) model of order one with constant. The PCF of Kafr Elzyat (Figure 8b.) behaves in the same manner as IGSR site

whereas ACF has spikes at lag 1 and 2 and cuts off after lag 1 and 2 (Figure 8a.). So the SO₂ data of Kafr Elzyat have an autoregressive model of order one and moving average of order two. By checking the autocorrelation functions of Mahala and Mansoura sites, it could be seen that, the SO₂ series of both are non stationary. So, ARIMA models of the first differenced SO₂ series of Mahala and Mansoura sites were identified by checking their ACFs (Figures.9a. and 10a.) and PCFs (Figures 9b. and 10b.). They all are presented in the Table 4.:

Table 4. ARIMA model for SO₂ of IGSR, Kafr Elzyat, Mahalla and Mansoura sites

Site	ARIMA (p,d,q)	Model
IGSR	(1,0,0)	$(1-\Phi_1B)X_t = a_t$
Kafr Elzyat	(1,0,2)	$(1-\Phi_1B)X_t = (1-\theta_1B - \theta_2B^2)a_t$
Mahalla	(1,1,1)	$(1-B)(1-\Phi_1B)X_t = (1-\theta_1B)a_t$
Mansoura	(0,1,2)	$(1-B)X_t = (1-\theta_1B - \theta_2B^2)a_t$

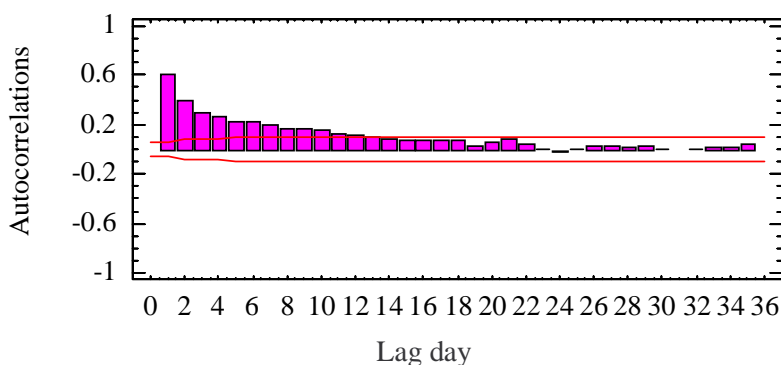


Figure 7a. ACF of daily average SO₂ for IGSR site during three years (2000-2002)

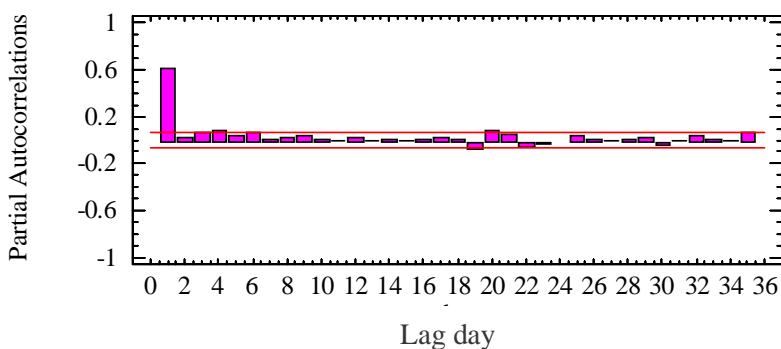


Figure 7b. PCF of daily average SO₂ for IGSR site during three years (2000-2002)

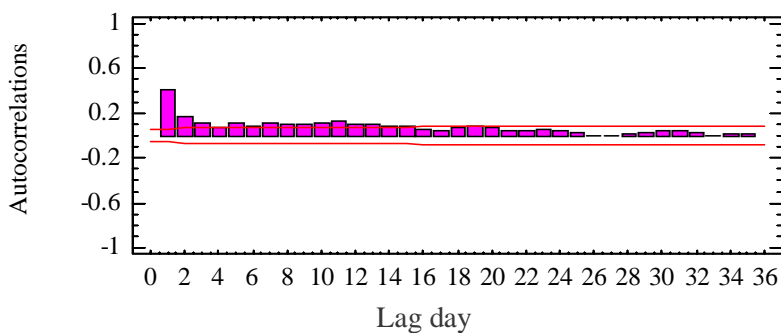


Figure 8a ACF of daily average SO₂ for Kafr Elzyat during three years (2000-2002)

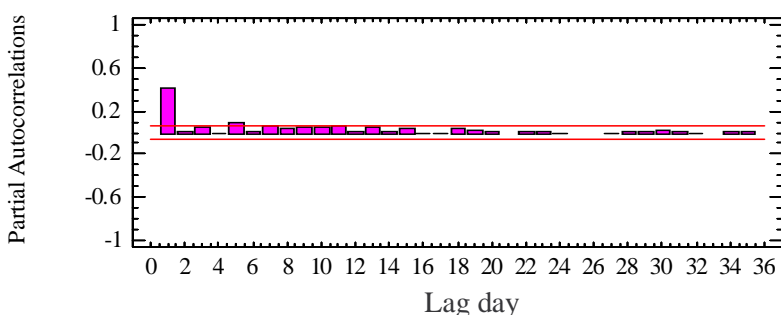


Figure 8b. PCF of daily average SO₂ for Kafr Elzyat during three years (2000-2002)

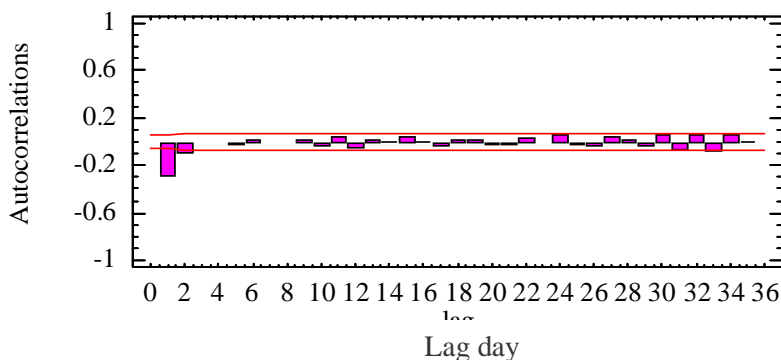


Figure 9a. ACF of daily average SO₂ after first difference for Mahalla site during three years

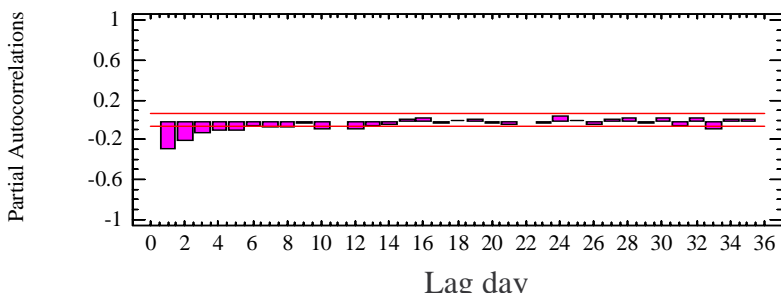


Figure 9b. PCF of daily average SO₂ after first difference for Mahalla site during three years

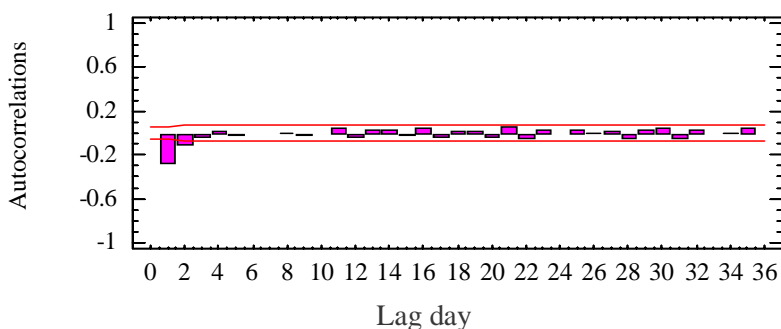


Figure 10a. ACF of daily average SO₂ after first difference at Mansoura site during three years (2000-2002)

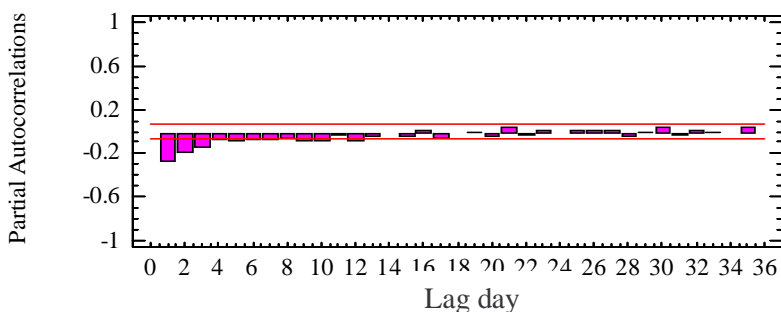


Figure 10b. PCF of daily average SO₂ after first difference at Mansoura during three years (2000-2002)

Ozone (O₃)

It is clear that the ACF of the time series values of O₃ dies down extremely slowly, and then the time series data should be considered non-stationarity. Hence, O₃ series must be transformed into stationarity series by making first difference. After making first difference stationarity is checked again by computing ACF as it is clear in Figure 11a. It is noticed that the ACF of the transformed data cuts off quickly, and then the transformed data should be considered stationarity. Now according to the Box -Jenkins methodology, the behavior of ACF and PCF were examined to specify general ARIMA model. The ACF has spikes at lag 1 and 2 days and cuts off after two days whereas the PCF dies down quickly as shown in Figures 11a. and 11b. Thus the O₃ series can be considered to follow the MA (2) (moving average) model of order two and difference of order one. Hence, the general ARIMA model is (0, 1, 2). $(1-B) X_t = (1-\theta_1 B - \theta_2 B^2) a_t$

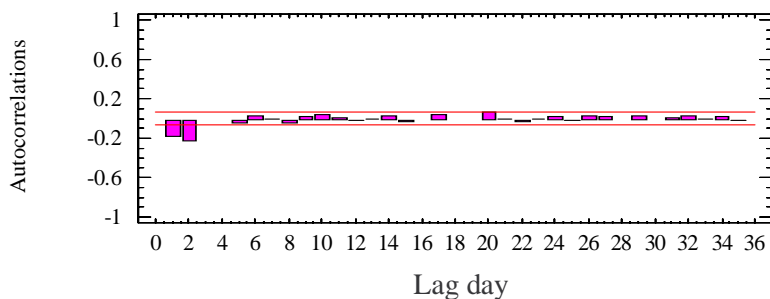


Figure 11a. ACF of daily average O₃ after first difference during three years (2000-2002)

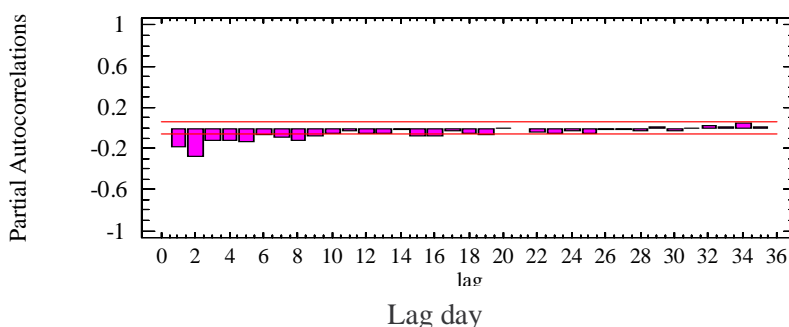


Figure 11b. PCF of daily average O₃ after first difference during three years (2000-2002)

Carbon monoxide (CO)

CO time series plots appear to be non stationary and needs to be transformed to stationary one. After that the ACF of the differenced CO data were computed, differenced data were found to have spikes at lag 1,2 and 3 and cuts off after lag 3, whereas the PCF dies down quickly as shown in Figures 12a. and 12b. Thus the CO series should follow the AR(3) (autoregressive) model of order three. So the general ARIMA model is $(0, 1, 3), (1-B) X_t = (1 - \theta_1 B - \theta_2 B^2 - \theta_3 B^3) a_t$ where, X_t = concentrations of CO.

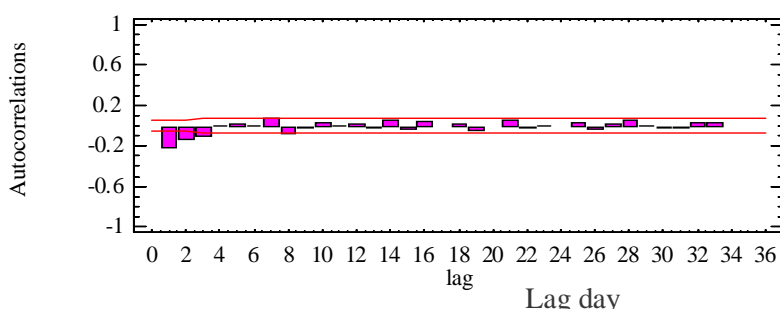


Figure 12a. ACF of daily average CO after first difference of IGSR site during three years (2000-2002)

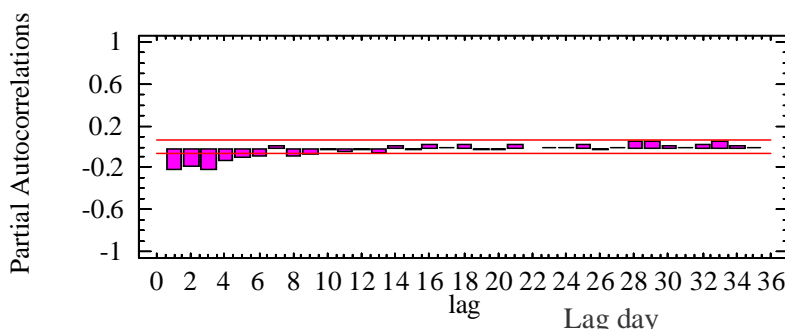


Figure 12b. PCF of daily average CO after first difference during three years (2000-2002)

(i) Model Estimation

The parameters of the models can be determined by the maximum likelihood or the least square methods. According to the former; the maximum likelihood estimates are calculated. Under the later method, those values of the parameters are chosen which will make the sum of the squared residual as small as possible. Their estimates were calculated with the aid of the Statistica software. The constant terms were excluded from the tentative ARIMA model

because the absolute t-value associated with the least squares point estimate of μ was not statistically different from zero ($p > 0.05$). The details of the model coefficients are listed in equations (1)-(12).

Particulate matter (PM₁₀)

$$\begin{aligned} Z_t &= 0.457Z_{t-1} + 0.092Z_{t-2} - 0.974a_{t-1} + a_t && \text{PM}_{10} \text{ of IGSR (1)} \\ Z_t &= 0.271Z_{t-1} - 0.767a_{t-1} - 0.167a_{t-2} + a_t && \text{PM}_{10} \text{ of Kafr Ezyat (2)} \\ Z_t &= a_t - 0.443a_{t-1} - 0.342a_{t-2} && \text{PM}_{10} \text{ of Mahalla (3)} \end{aligned}$$

Nitrogen dioxide (NO₂)

$$\begin{aligned} Z_t &= a_t - 0.526a_{t-1} - 0.249 a_{t-2} && \text{NO}_2 \text{ of IGSR (4)} \\ Z_t &= 0.352Z_{t-1} - 0.884a_{t-1} + a_t && \text{NO}_2 \text{ of Kafr Ezyat (5)} \\ Z_t &= a_t - 0.909X_{t-1} - 0.585Z_{t-2} - 0.448Z_{t-3} - 0.305Z_{t-4} - 0.200Z_{t-5} + 0.412a_{t-1} && \text{NO}_2 \text{ of Mansoura (6)} \end{aligned}$$

Sulfur dioxide (SO₂)

$$\begin{aligned} X_t &= 11.6 + 0.61 X_{t-1} + a_t && \text{SO}_2 \text{ of IGSR (7)} \\ X_t &= 29.54 + 0.96X_{t-1} - 0.58a_{t-1} - 0.28a_{t-2} + a_t && \text{SO}_2 \text{ of Kafr Ezyat (8)} \\ Z_t &= 0.47X_{t-1} - 0.23a_{t-1} + a_t && \text{SO}_2 \text{ of Mahalla (9)} \\ Z_t &= a_t - 0.44a_{t-1} - 0.23a_{t-2} && \text{SO}_2 \text{ of Mansoura (10)} \end{aligned}$$

Ozone (O₃)

$$Z_t = a_t - 0.439a_{t-1} - 0.280a_{t-2} \quad \text{O}_3 \text{ of Alexreginal (11)}$$

Carbon monoxide (CO)

$$Z_t = a_t - 0.417a_{t-1} - 0.230a_{t-2} - 0.133a_{t-3} \quad \text{CO of IGSR (12)}$$

(ii) Model Diagnostic

The statistical adequacy of the model is next verified by various diagnostic checks. This is primarily done by residual analysis. If the model is properly specified then, the residuals in the model should behave as white noise and be uncorrelated. Therefore, model inadequacy can be evaluated by examining a residual plot and the autocorrelation functions of the residuals. In this study the model tested by making (1) Independence (2) Normality (3) Constancy of the variance

- **Independence**

To check whether the residuals (errors) are uncorrelated, we compute the sample autocorrelation of the residuals to see whether they do not form any pattern and are all statistically insignificant. There are no statistically significant correlations at 95% in the ACF and PACF residuals of the specified models. Therefore, the residuals can be considered as white noise.

- **Normality**

To check whether the residuals are normality distributed or not, one can construct a histogram of the residuals and compare it with the standard normal distribution. Normality can be checked more carefully by plotting the so called normal plot test of the residuals. The

ARIMA model assumes that the residuals are normally distributed. Generally the residual distributions of all ARIMA series could be considered as normal distribution.

- **Constancy of the variance**

In order check the validity of the constant variance assumption, we plot the residuals against time (scatter plot). If the residual plots have a horizontal band appearance, we conclude that there is no evidence of a violation of the constant variance assumption. Moreover an examination of residuals over time can often indicate whether the modeling technique being used does or does not match this pattern. It is important to measure the magnitude of errors so that we can determine whether accurate forecasting is possible. In order to do this, we might consider the mean sum of squares of all forecast errors (MSE) over time.

The residual variance of ARIMA series shows that they are nearly constant. This indicates that the trend and seasonality are adequately modeled, although they contain some outliers. From the residual analysis of all series, it can be concluded that, the residuals of the ARIMA models are uncorrelated and thereby the final models of the series can be presented as in equations (1)-(12). Figures 13. through 17. reveal the actual and forecast series for PM₁₀, NO₂, SO₂, O₃ and CO, respectively.

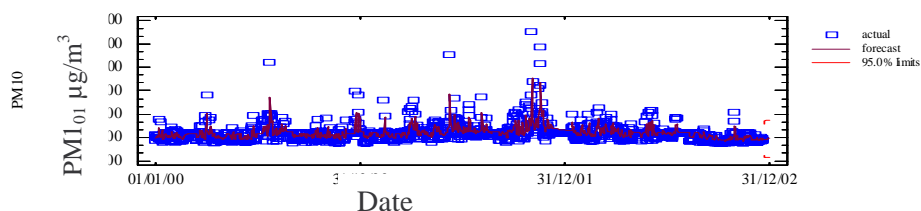


Figure 13a. Plot of actual and forecast ARIMA (2, 1, 1) PM₁₀ series of IGSR.

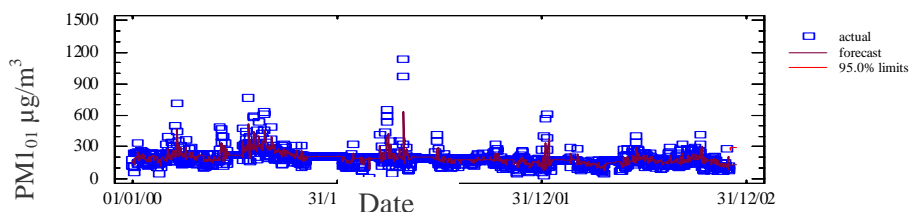


Figure 13b. Plot of actual and forecast ARIMA(1,1,2) PM₁₀ series of Kafr Elzyat .

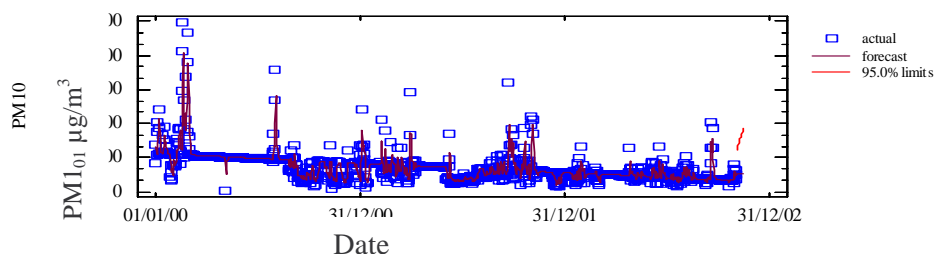


Figure 13c. Plot of actual and forecast ARIMA (0, 1, 2) PM₁₀ series of Mahalla

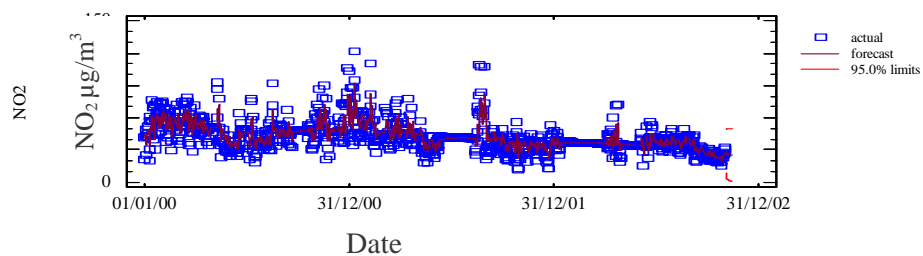


Figure 14a. Plot actual and forecast ARIMA (0, 1, 2) NO₂ series of IGSR.

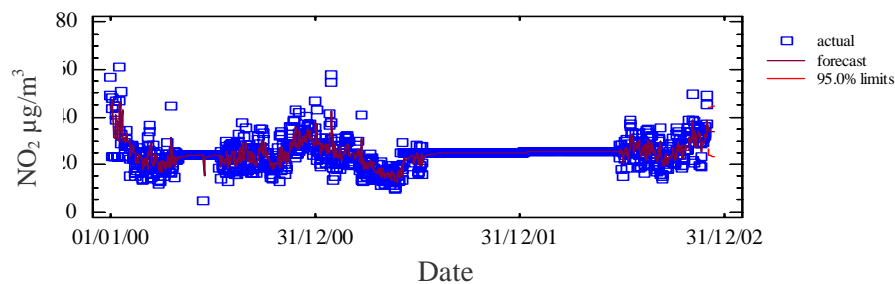


Figure 14b. Plot actual and forecast ARIMA (1, 1, 2) NO₂ series of Kafr Elzyat site

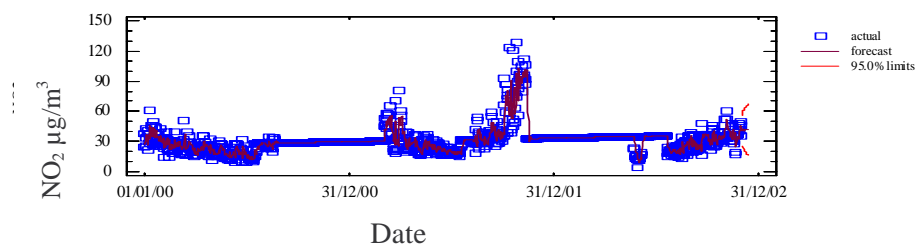


Figure 14c. Plot actual and forecast ARIMA (5, 1, 1) NO₂ series of Mansoura site

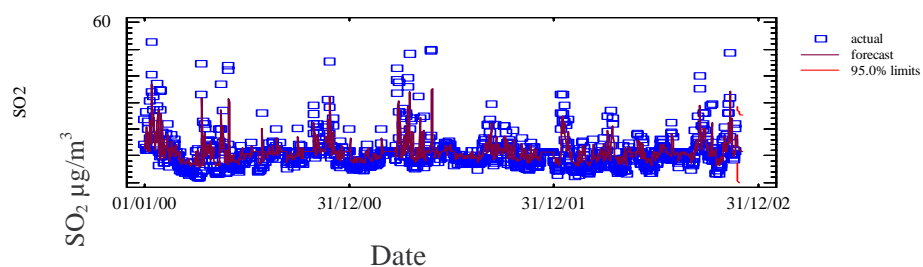


Figure 15a. Plot of actual and forecast ARIMA (1, 0, 0) SO₂ series for IGSR site.

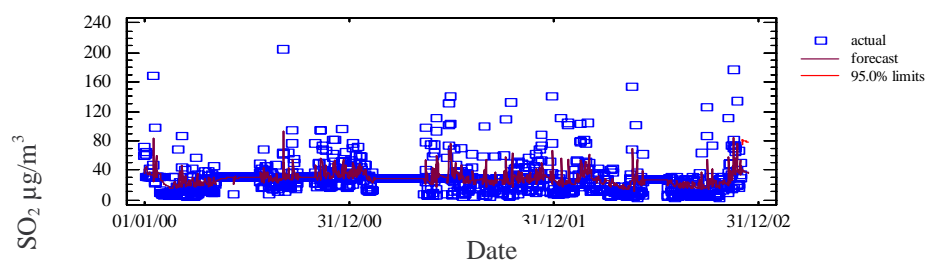


Figure 15b. Plot of actual and forecast ARIMA (1, 0, 2) SO₂ (µg/m³) series for Kafr Elzyat site.

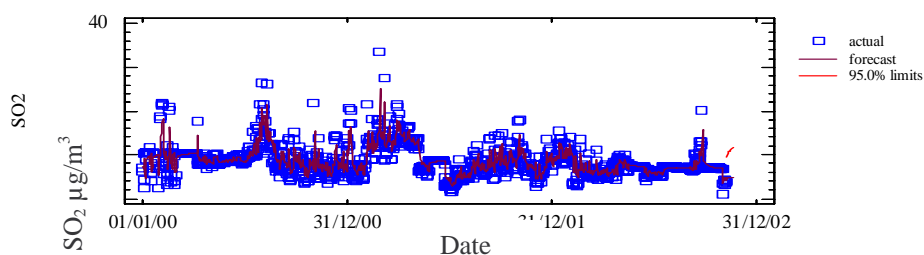


Figure 15c. Plot of actual and forecast ARIMA(1,1,1) SO₂ series for Mahalla site .

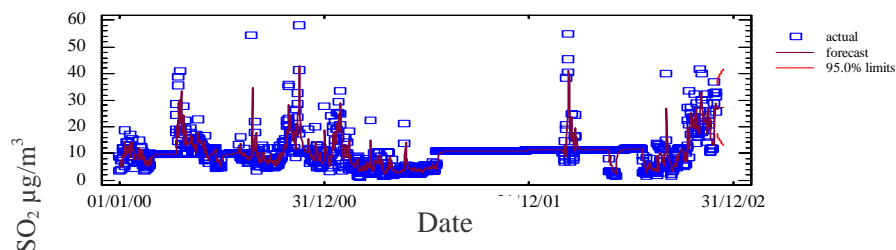


Figure 15d. Plot of actual and forecast ARIMA (0, 1, 2) SO₂ series for Mansoura site.

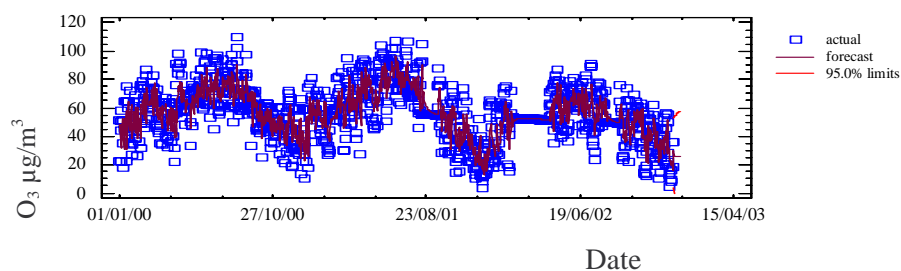


Figure 16. Plot actual and forecast ARIMA (0, 1, 2) O₃ series.

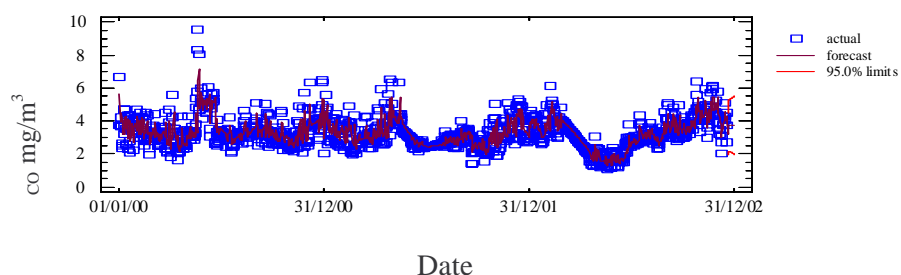


Figure 17. Plot of actual and forecast ARIMA (0, 1, 3) CO series.

Cross Correlations of Pollutants: Sulfur dioxide (SO₂) and Particulate matter (PM₁₀)

The cross correlation between daily SO₂ and PM₁₀ concentrations at IGSR site demonstrates a significant positive correlation value of 0.15 at lag 1 and a little correlation of 0.07 at zero lag as shown in Figure 18a. This means that, after one day SO₂ makes significant increase in PM₁₀ concentrations. This behavior presents emphasis on solid phase reaction of SO₂ on particulate matter which is alkaline in nature making conditions conducive for formation of SO₄²⁻, where CaCO₃ is the main component of the soil (Shalaby, 1997). In the case of calcium carbonate, the reaction of SO₂ is thermodynamically favorable (Usher et al., 2002), so the alkaline nature of particles offers the preferable oxidation of acidic SO₂ gas on

the dust particles during suitable meteorological conditions (Kulshrestha et al., 2003) as follows:



The plot of CCF (cross correlation function) between daily SO₂ and PM₁₀ concentrations of Mahalla site depicts a significant value (0.4) at lag 0 on 95% level. This correlation indicates that, SO₂ and PM₁₀ share the same source. The situation is different in case of Kafr Elzyat, where the cross correlation between daily SO₂ and PM₁₀ concentrations shows no significant correlation coefficients at 95% level. This means that, SO₂ and PM₁₀ have different sources, where Fertilizer Company emits NO₂ and SO₂ and brick factories emit SO₂ and PM₁₀.

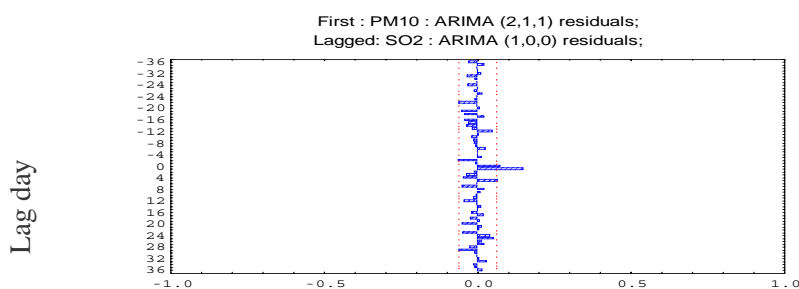


Figure 18a. Plot of cross correlation between SO₂ and PM₁₀ residuals at IGSR site

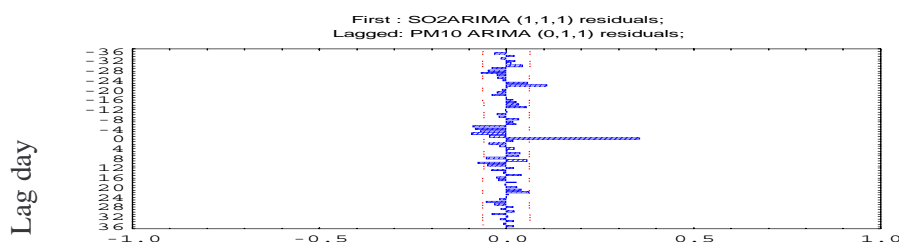


Figure 18b. Plot of cross correlation between SO₂ and PM₁₀ of Mahalla site (2000-2002)

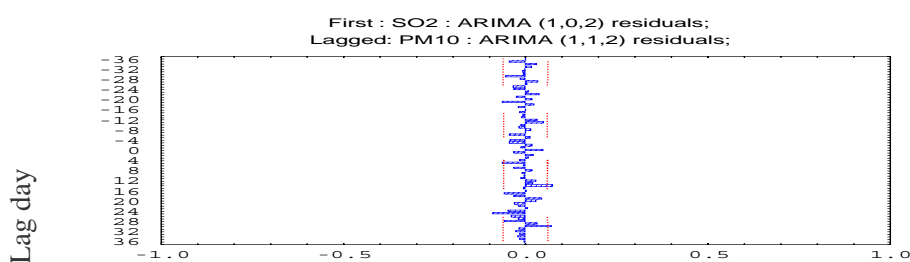


Figure 18c. Plot of cross correlation between daily SO₂ and PM₁₀ residuals at Kafr Elzyat

Sulfur dioxide (SO₂) and Ozone (O₃)

Oxidation of adsorbed SO₂ by Gas phase ozone

Figure 19. shows that the concentrations of daily SO₂ at IGSR site were negatively correlated with daily O₃ concentrations especially at time lag 0 and 1. This suggests that, the amount of deposited O₃ was used for oxidation of S (IV) to S (VI) (Sakamoto at al., 2004). The oxidation of adsorbed SO₂ with ozone on several oxides Fe₂O₃, Al₂O₃, and MgO, was investigated. The conversion of chemisorbed sulfite/bi-sulfite to sulfate/bisulfate is evident in literature (Usher et al., 2002).



At high pH values, metal ion oxidation of sulfur by O₂ is controlled, and oxidation by dissolved O₃ is favored (Liang and Jacobson, 1999). Thus, we believe that when the particulate surface has a high pH, oxidation by O₃ predominates. There are several plausible mechanisms for sulfur oxidation by O₃, but here we will mention the most important one which is radical SO₂ with radicals produced by the decomposition of O₃. Ozone is reportedly decomposed by mineral dust containing mineral oxides such as SiO₂, Fe₂O₃, and Al₂O₃ (Hanisch and Crowley, 2003), so O₃ may be completely decomposed, as the particles contain these metallic elements (Sakamoto et al., 2004). From the above mentioned consideration, it may be thought that, the oxidation of SO₂ by O₃ occurred by means of a heterogeneous reaction on the particle surface:



Furthermore, the moisture absorbed onto the particulate surface (especially under wet conditions) enhanced the oxidation by O₃ (Dentener et al., 1996 and Usher et al., 2002):

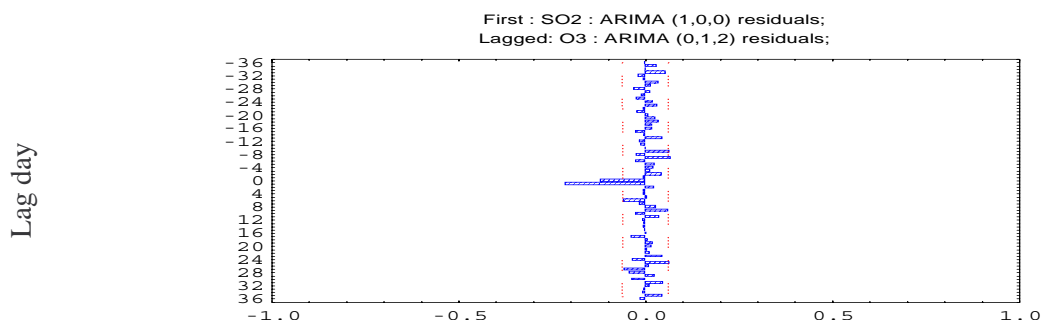


Figure 19. Plot of cross correlation between daily SO₂ and O₃ residuals at IGSR site.

Sulfur dioxide (SO₂) and Nitrogen dioxide (NO₂)

CCF between SO₂ and NO₂ of IGSR site (Figure 20a.) depicts a statistically significant correlation at zero lag (0.4) that further supports that mobile sources are contributing to SO₂ pollution at IGSR site (Aneja et al., 2001).

Figure 20b. demonstrates the cross correlations between SO₂ and NO₂ at Kafr Elzyat site. It reveals a positive correlation (0.228) at lag 0. This good correlation over all measurement period suggests a common origin for both pollutants, such as brick factories, fertilizer factories and vehicle emissions. Cross correlation of Mansoura between ARIMA (2, 1, 1) NO₂ and ARIMA (0, 1, 2) SO₂ time series residuals of Mansoura site were performed and graphed in Figure 20c. It is obvious that there is a statistically significant positive correlation at lag 0 (0.2). This indicates that, they have common sources and that NO₂ partially has primary sources in Mansoura region.

Carbon monoxide (CO) and Nitrogen dioxide (NO₂)

The cross correlation between daily time series residuals (0, 1, 2) of NO₂ and (0, 1, 3) of CO gives a statistically significant positive correlation at time lag one (0.23) as shown in Figure 21. This could be explained by the fact that NO reacts with proxy radicals which are formed from the oxidation of CO and hydrocarbons by OH attack and is converted to NO₂ (Aneja et al., 1997) which is highly consistent with the ratio characteristic of road traffic

emissions (Cardenas et al., 1998). This proves that, motor vehicle exhaust is the primary sources of most of CO concentrations at IGSR site.

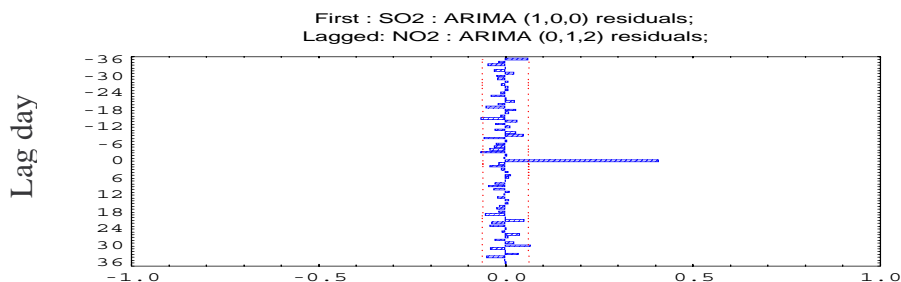


Figure 20a. Plot of cross correlation between SO₂ and NO₂ residuals at IGSR site

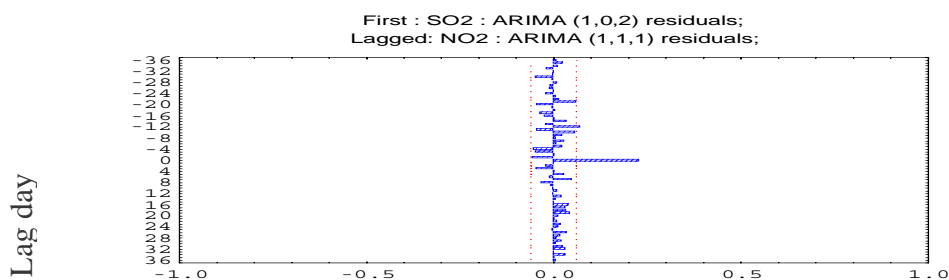


Figure 20b. Plot of cross correlation between SO₂ and NO₂ residuals at Kafr Elzyat site

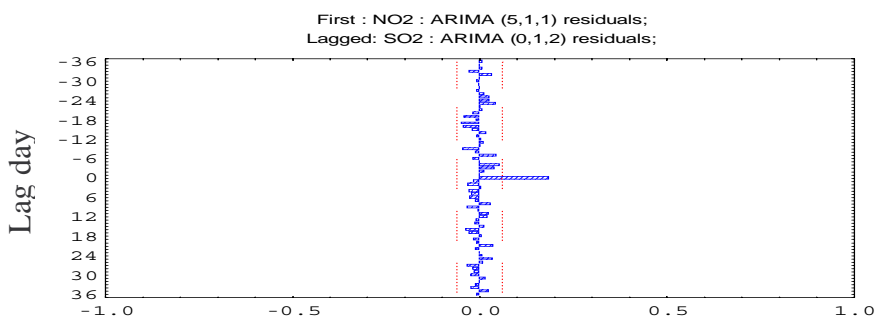


Figure 20c. Plot of cross correlation between SO₂ and NO₂ residuals at Mansoura site

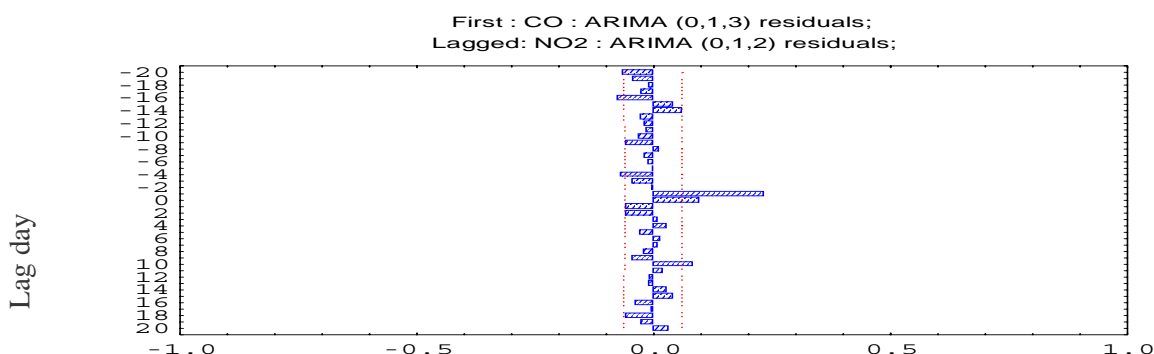


Figure 21. Plot of cross correlation between daily NO₂ and CO of IGSR site (2000-2002).

Nitrogen dioxide (NO₂) and Ozone (O₃)

Cross correlation function plot between NO₂ and O₃ has been depicted in Figure 22. It reveals a significant negative correlation of -0.21 and -0.15 at lag 0 and 1. This result is

expected since O₃ production is dependant on NO₂ concentrations. The production of O₃ is a complex function of NO_x concentrations, concentrations and reactivity of hydrocarbons, light intensity, temperature etc. In the polluted troposphere, O₃ is generated by a non linear photochemical system. In the presence of water vapors, the hydroxyl radicals OH is produced through the reaction of H₂O with excited oxygen. The hydroxyl radical attacks VOCs and leads to formation of organic peroxy radicals. The peroxy radicals then oxidize NO to NO₂, followed by photo dissociation of NO₂ and production of atomic oxygen. Atomic oxygen in turn combines with molecular oxygen to form O₃. In other words, on the time scale of minutes, practically all of the local NO₂ in the troposphere has been produced at the expense of O₃ (Derwent, 1990).

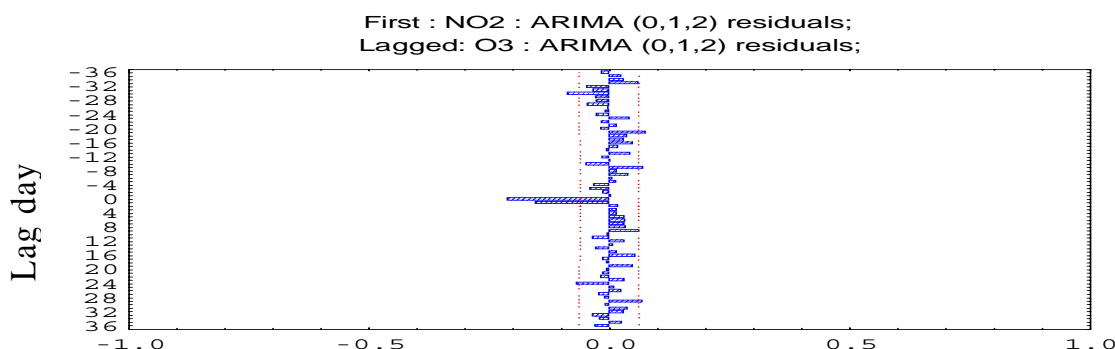


Figure 22. Plot of cross correlation between daily NO₂ and O₃ of IGSR site (2000-2002).

Carbon monoxide (CO) and Ozone (O₃)

The cross correlation of daily time series residuals (0, 1, 2) O₃ and (0, 1, 3) CO was investigated and a statistically significant negative correlation (-0.40) was noticed at zero time lag (Figure 23). The anti correlation between CO and O₃ could be explained by the fact that, HO₂ is produced in the oxidation of CO to CO₂ and leading to additional ozone formation (Aneja et al., 1997). Also a negative correlation indicates that, the pollution source was very close (Kato et al., 2004). In the presence of high NO concentrations the HO₂ product of CO destruction loses an oxygen atom to form NO₂, which rapidly dissociates to form ozone. In the absence of NO_x, the HO₂ molecule reacts directly to destroy O₃. In practice, the change in CO would be inversely proportional to the increase in OH in the condition of methane oxidation is small and when there is no local sink due to advection (Holloway et al., 2000)

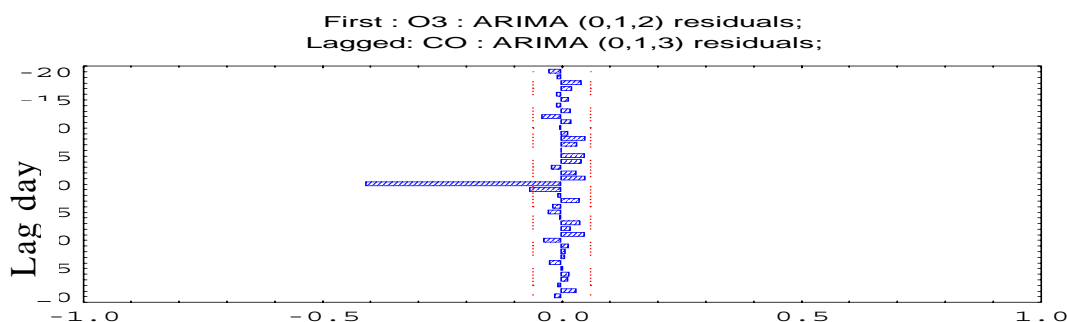
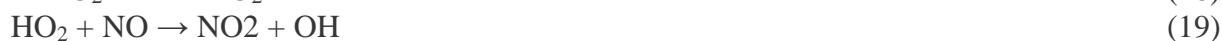


Figure 23. Plot of cross correlation of daily O₃ and CO at IGSR site.

CONCLUSION

1. Autocorrelations and cross correlation analysis of long term monitoring time series of air pollution indicators has revealed important information on the dynamics, chemistry and interpretation of ambient pollution such as the low levels of SO₂.
2. Sulfur dioxide levels in ambient air are not true indicators of sulfur pollution.
3. Statistical analysis of nitrogen dioxide concentrations at Mansoura site indicates that it has different behavior than other sites, which results from the existence of fertilizer factory there.

RECOMMENDATIONS

1. Extensive study should be carried out at Mansoura site especially for NO₂, where the time series analysis gives different results from other sites.
2. It is recommended to measure sulphate ion concentration as well as SO₂.
3. The encouraging results obtained in this work suggest continuing work to produce multiple time series models to achieve better forecasting results.

REFERENCES

1. Kolehmainen M., Martikainen H. and Ruuskanen J., (2001). Neural networks and periodic components used in air quality forecasting. *Atmospheric Environment* 35, 815-825.
2. Kukkonen J., Partanen I., Karppinen A., Ruuskanen J., Junninen H., Kolehmainen M., Niska H., Dorling S., Chatterton T., Foxall R. and Cawley G., (2003). Extensive evaluation of neural network models for the prediction of NO₂ and PM₁₀ concentrations, compared with a deterministic modeling system and measurements in central Helsinki. *Atmospheric Environment* 37, (32), 4539-4550.
3. Milionis; A.E. and Davies; T.D., 1994; Regression and stochastic models for air pollution. Review, comments and suggestions; *Atmospheric Environment* 28,(17), 2801-2810.
4. Box G.E.P. and Jenkins G.M., (1970). *Time series analysis: Forecasting and control*. Holden Day, San Francisco.
5. Shalaby E.A., (1997). Assessment of Cd, Pb, and Zn in aerosol, soils and leaves of Ficus SPP, and Eucalyptus SPP. Trees in some regions of western area of Nile delta. *Journal of Agriculture Science, Mansoura University*, 22(12), 4771-4782.
6. Usher C.R., Al Hosney H., Carlos-Cuellar S. and Grassian V.H., (2002); A laboratory study of the heterogeneous uptake and oxidation of sulfur dioxide on mineral dust particles; *Journal of Geophysical research* 107, 4713 DOI 10.1029/2002 JD002051.
7. Kulshrestha M. J., Kulshrestha U. C., Parashar D.C. and Vairamani M., (2003); Estimation of SO₄ contribution by dry deposition of SO₂ onto the dust particles in India. 37, 3057-3063.
8. Sakamoto K., Takada H. and Sekiguchi K., (2004). Influence of ozone, relative humidity, and flow rate on the deposition and oxidation of sulfur dioxide on yellow sand. *Atmospheric Environment* 38, 6961-6967

9. Liang J. and Jacobson M.Z., (1999). A study of sulfur dioxide oxidation pathways over a range of liquid water contents, pH Journal of Geophysical research values and temperature. Journal of Geophysical research 104, 13749-13769.
10. Hanisch F. and Crowley J.N., (2003). Ozone decomposition on Saharan dust: an experimental investigation; Atmospheric Chemistry and physics 3, 119-130.
11. Dentener F.J., Carmichael G.R., Zhang Y., Lelieveld J. and Crutzen P.J., (1996) Dr. M. El Raey 4/25/2006); Role of mineral aerosol as a reactive surface in the global troposphere; Journal of Geophysical research 101, 22869-22889
12. Aneja V. P., Agarwal A., Roelle P. A., Phillips S. B., Tong Q., Watkins N. and Yablonsky R., (2001); Measurements and analysis of criteria pollutants in New Delhi, India. Environment International, 27, 35-42.
13. Aneja V. P., Kim D. S. and Chameides W. L., (1997). Trends and analysis of ambient NO, NO_y, CO, and ozone concentrations in Raleigh, North Carolina; Chemosphere 34, (3), 611-623.
14. Cardenas L.M., Austin J.F., Burgess R.A., Clemitshaw K.C., Dorling S., Penkett S.A. and Harrison R.M., (1998). Correlations between CO, NO_y, O₃ and non methane hydrocarbons and their relations with meteorology during winter 1993 on the north Norfolk coast, U.K. Atmospheric Environment 32,(19), 3339-3351.
15. Derwent R.G., (1990); Evaluation of a number of chemical mechanisms for their application in models describing the formation of photochemical ozone in Europe; Atmospheric Environment 24A, (10), 2615-2624
16. Kato S., Kajii Y., Itokazu R., J Hirokawa J., S Koda S. and Kinjo Y., (2004). Transport of atmospheric carbon monoxide, ozone and hydrocarbons from Chinese coast to Okinawa Island in the Western Pacific during winter Dr. M. El Raey 4/25/2006; Atmospheric Environment 38, (19), 2975-2981.
17. Holloway T., Levy H. and Kasibhatla P., (2000); Global distribution of carbon monoxide. Journal of geophysical research 105, D01, 12,123-12,147